Biochimica et Biophysica Acta 1830 (2013) 2178–2187

Contents lists available at SciVerse ScienceDirect

Biochimica et Biophysica Acta

journal homepage: www.elsevier.com/locate/bbagen

Broad-complex functions in postembryonic development of the cockroach *Blattella germanica* shed new light on the evolution of insect metamorphosis

Jia-Hsin Huang [1], Jesus Lozano, Xavier Belles *

Institute of Evolutionary Biology (CSIC-Universitat Pompeu Fabra), Passeig Marítim de la Barceloneta 37, 08003 Barcelona, Spain

ARTICLE INFO

Article history:
Received 1 August 2012
Received in revised form 27 September 2012
Accepted 28 September 2012
Available online 3 October 2012

Keywords:
Insect metamorphosis
Juvenile hormone
Ecdysone
Evolution of holometaboly
Drosophila
Tribolium

ABSTRACT

Background: Insect metamorphosis proceeds in two modes: hemimetaboly, gradual change along the life cycle; and holometaboly, abrupt change from larvae to adult mediated by a pupal stage. Both are regulated by 20-hydroxyecdysone (20E), which promotes molts, and juvenile hormone (JH), which represses adult morphogenesis. Expression of Broad-complex (BR-C) is induced by 20E and modulated by JH. In holometabolous species, like *Drosophila melanogaster*, BR-C expression is inhibited by JH in young larvae and enhanced in mature larvae, when JH declines and BR-C expression specifies the pupal stage.
Methods: Using *Blattella germanica* as a basal hemimetabolous model, we determined the patterns of expression of BR-C mRNAs using quantitative RT-PCR, and we studied the functions of BR-C factors using RNA interference approaches.
Results: We found that BR-C expression is enhanced by JH and correlates with JH hemolymph concentration. BR-C factors appear to be involved in cell division and wing pad growth, as well as wing vein patterning.
Conclusions: In *B. germanica*, expression of BR-C is enhanced by JH, and BR-C factors appear to promote wing growth to reach the right size, form and patterning, which contrast with the endocrine regulation and complex functions observed in holometabolous species.
General significance: Our results shed new light to the evolution from hemimetaboly to holometaboly regarding BR-C, whose regulation and functions were affected by two innovations: 1) a shift in JH action on BR-C expression during young stages, from stimulatory to inhibitory, and 2) an expansion of functions, from regulating wing development, to determining pupal morphogenesis.

1. Introduction

The origin and evolution of insect metamorphosis poses one of the most enigmatic conundrums in evolutionary biology. In his "On the Origin of Species", Charles Darwin already complained about the difficulty of integrating insect metamorphosis (due to the striking difference between the morphologies and life styles of larvae and adults of the same species) into his theory of species evolution by natural selection [1]. However, it is clear that insect metamorphosis has been a key innovation in insect evolution as most of the present biodiversity on Earth is composed of metamorphosing insects, with approximately 1 million species described, and 10–30 million still to be discovered [2,3].

The first systematic studies on insect metamorphosis were carried out by Renaissance entomologists, who established that post-embryonic changes are most spectacular in insects like butterflies, beetles and flies, which undergo a dramatic morphological transformation from larva to pupa and adult, a phenomenon now known as holometaboly. Other insects, such as locusts and cockroaches, also metamorphose from the last nymphal instar to adult, although the change of form is not as radical given that the nymphs are similar to the adults. However, they undergo qualitative metamorphic changes, such as formation of mature wings and external genitalia in a type of metamorphosis known as hemimetaboly [4,5]. Metamorphosis evolved from hemimetaboly to holometaboly, and the latter innovation was most successful because more than 80% of present insects are holometabolous species (including the "big four" orders: Lepidoptera, Coleoptera, Diptera and Hymenoptera) [2,3]. Therefore, explaining the evolutionary transition from hemimetaboly to holometaboly may give a new look to explain how this amazing biodiversity originated, and the study of the processes regulating metamorphosis shall surely provide important clues for such a goal [6].

Insect metamorphosis is regulated by two hormones, the molting hormone, which promotes molting, and the juvenile hormone (JH), which represses metamorphosis and, thus determines the molt type: to an immature stage when it is present, or to the adult when it is absent [4,6,7]. Although the molecular action of JH is still poorly understood [8], we know that an important transducer of the JH signal is Methoprene tolerant (Met), a transcription factor that was discovered in *Drosophila*

* Corresponding author. Tel.: +34 932309636; fax: +34 932211011.
E-mail address: xavier.belles@ibe.upf-csic.es (X. Belles).
[1] Permanent address: Department of Entomology, National Taiwan University, Taipei 106, Taiwan.

0304-4165/$ – see front matter © 2012 Elsevier B.V. All rights reserved.
http://dx.doi.org/10.1016/j.bbagen.2012.09.025

melanogaster and that plays an important role in JH reception [9]. Key functional evidence that Met is required for the repressor action of JH on metamorphosis was obtained from the beetle *Tribolium castaneum*, a basal holometabolous insect where depletion of Met expression induced larvae to undergo precocious metamorphosis [10,11]. More recently, the function of Met as an early JH transducer has been demonstrated in the hemimetabolous species *Pyrrhocoris apterus* [12], which established the first regularity in the signaling pathway of JH in hemimetabolous and holometabolous insects. Another important element in JH transduction in relation to metamorphosis is the transcription factor Krüppel homolog 1 (Kr-h1), whose antimetamorphic action was firstly demonstrated in *D. melanogaster* [13] and *T. castaneum* [14]. More recently, the role of Kr-h1 as a transducer of the JH signal has been reported in three hemimetabolous insects: the cockroach *Blattella germanica* [15] and the bugs *P. apterus* and *Rhodnius prolixus* [12]. RNAi studies in these species have shown that Kr-h1 represses metamorphosis and that it acts downstream of Met in the JH signaling pathway. Kr-h1 therefore appears to be the more distal transcription factor in the JH signaling cascade whose role as mediator of the antimetamorphic action of JH has been conserved from cockroaches to flies. The next challenge is to unveil the factor(s) specifying the adult stage that are repressed by Kr-h1.

Concerning the molecular action of molting hormones, the effect of 20-hydroxyecdysone (20E) is also mediated by a cascade of transcription factors that starts upon its binding to the heterodimeric receptor composed of the ecdysone receptor and the ultraspiracle, which belong to the nuclear receptor superfamily. This activates expression of a hierarchy of transcription factors generally belonging to the same superfamily, like E75, E78, HR3, HR4 and FTZ-F1, which regulate the genes that underlie the cellular changes associated to molting and metamorphosis [16,17]. Most of the information available on this cascade refers to *D. melanogaster* [18,19], but there are a good deal of data from hemimetabolous species, especially from the cockroach *B. germanica*. Factors involved in 20E signaling in *B. germanica* are generally the same as in *D. melanogaster*, although the functions of some of them and their epistatic relationships may differ with respect to those observed in the fly [20–22].

Among the most interesting 20E-dependent factors are the products of the Broad-complex (BR-C) gene, whose functions may have radically diverged in hemimetabolous and holometabolous species. BR-C encodes a group of C2H2 zinc-finger transcription factors [23,24] that, in holometabolous species, like the dipteran *D. melanogaster*, the lepidopterans *Manduca sexta* and *Bombyx mori*, and the coleopteran *T. castaneum*, are expressed in the final larval stage, and this transient expression is essential for the successful formation of the pupae [11,25–28]. Experiments carried out on the hemipterans *Oncopeltus fasciatus* [29] and *P. apterus* [12], which are phylogenetically distal hemimetabolous species, suggested that BR-C transcription factors only regulate gradual wing bud growth. This specific role, which is radically different from the morphogenetic functions involved in pupae formation in holometabolous species, prompted us to undertake a detailed functional study of BR-C in *B. germanica*, a basal polyneopteran insect representing a poorly modified hemimetabolous species [4]. In *B. germanica*, the BR-C gene encodes six zinc-finger isoforms (BR-C Z1 to Z6), which play important roles in embryogenesis [30]. The present work, based on functional studies in post-embryonic development, reveals ancestral functions of BR-C transcription factors related to cell division and of wing pad growth, as well as to wing vein patterning, and provides new clues that illuminate the evolution of insect metamorphosis.

2. Materials and methods

2.1. Insects

B. germanica specimens used in the experiments were obtained from a colony reared in the dark at 30 ± 1 °C and 60–70% r.h. They were carbon dioxide-anesthetized prior to dissections and tissue sampling.

2.2. RNA extraction and retrotranscription to cDNA

All RNA extractions were carried out with the Gen Elute Mammalian Total RNA kit (Sigma-Aldrich, Madrid, Spain). An amount of 400 ng from each RNA extraction was treated with DNase (Promega, Madison, WI, USA) and reverse transcribed with Superscript II reverse transcriptase (Invitrogen, Carlsbad, CA, USA) and random hexamers (Promega). RNA quantity and quality were estimated by spectrophotometric absorption at 260 nm in a Nanodrop Spectrophotometer ND-1000® (NanoDrop Technologies, Wilmington, DE, USA).

2.3. Determination of mRNA levels with quantitative real-time PCR

Quantitative real time PCR (qRT-PCR) reactions were carried out in triplicate in an iQ5 Real-Time PCR Detection System (Bio-Rad Laboratories, Madrid, Spain), using SYBR®Green (Power SYBR® Green PCR Master Mix; Applied Biosystems, Madrid, Spain). A control without a template was included in all batches. The primers used to detect all isoforms simultaneously or to detect each isoform specifically are described in Table S1 (see Supplementary data). The efficiency of each primer set was first validated by constructing a standard curve through four serial dilutions. mRNA levels were calculated relative to BgActin-5c (accession number: AJ862721) expression using the Bio-Rad iQ5 Standard Edition Optical System Software (version 2.0). The primers used to quantify BgActin-5c are indicated in Table S2 (see Supplementary data). We followed a method based in Ct (threshold-cycle) according to the Pfaffl mathematical model [31], simplifying to $2^{\Delta\Delta Ct}$ because the calculated efficiency values for studied genes and BgActin-5c amplicons were always within the range of 95 to 100%; therefore, no correction for efficiency was used in further calculations. Results are given as copies of mRNA per 1000 copies of BgActin-5c mRNA.

2.4. Treatments with juvenile hormone III in vivo

To study the effect of JH upon BR-C expression, JH III, which is the native JH of *B. germanica* [32,33], was applied topically to freshly emerged last instar nymphs at a dose of 20 μg per specimen in 1 μl of acetone. We used JH III from Sigma-Aldrich, which is a mixture of isomers containing about 50% of the biologically active (10R)-JH III. Thus, the active dose applied would be around 10 μg per specimen, which is an efficient dose to impair metamorphosis [34]. Controls received 1 μl of acetone.

2.5. RNA interference

B. germanica is very sensitive to RNA interference (RNAi) in vivo [35]. Detailed procedures for dsRNA preparation and RNAi experiments were as described previously [22,36,37]. Concerning BR-C, dsRNAs were prepared to deplete all isoforms simultaneously (dsBrCore) or specific isoforms BR-C Z1 to BR-C Z6 (dsBrZ1 to dsBrZ6). The primers used to generate templates with PCR for transcription of these dsRNAs are described in Table S3 (see Supplementary data). The fragments were amplified by PCR and cloned into the pSTBlue-1 vector (Novagen, Madrid, Spain). In all cases, we used a 307 bp sequence from *Autographa californica* nucleopolyhydrosis virus (accession number: K01149, from nucleotides 370 to 676) as control dsRNA (dsMock). A volume of 1 μl of each dsRNA solution (3 μg/μl) was injected into the abdomen of specimens at chosen ages and stages. The control specimens were treated with the same dose and volume of dsMock. RNAi of Kr-h1was carried out as recently reported [15].

2.6. Wing morphological studies

Development of mesonotum and metanotum wing primordia or wing buds was studied in 5th (N5, penultimate) and 6th (N6, last) nymphal instars. Wing buds were exposed out of the dorsal cuticular layer under Ringer's saline. Then, they were fixed in 4% paraformaldehyde and permeabilized in PBS-0.2% tween (PBT), incubated for 20 min in 300 ng/ml phalloidin–tetramethylrhodamine isothiocyanate (Sigma-Aldrich) in PBT, rinsed with PBS, and stained for 10 min in 1 μg/ml DAPI in PBT. After three washes with PBT, the wing buds were mounted in Mowiol 4–88 (Calbiochem), and were examined by epifluorescence microscopy AxioImager.Z1 (ApoTome System, Zeiss). Adult forewings (tegmina) and hindwings (membranous) were studied and photographed first in the intact animal, and then dissected out, mounted on a slide with Mowiol 4–88. In these cases, examinations and photographs were made with a stereomicroscope Zeiss DiscoveryV8. Biometrical measurements of wing size parameters were carried out with an ocular micrometer adapted to this stereomicroscope.

2.7. EdU experiments to measure cell proliferation in vivo

EdU (5-ethynyl-2′-deoxyuridine) is a thymidine analogue recently developed for labeling DNA synthesis and dividing cells in vitro [38,39], which is more sensitive and practical than the commonly used 5-bromo-2′-deoxyuridine, BrdU. We followed an approach in vivo, using the commercial EdU compound "Click-it EdU-Alexa Fluor® 594 azide" (Invitrogen, Molecular Probes), which was applied topically on the first abdominal tergites (10 μg in 1 μl of DMSO) of staged nymphs. The control specimens received 1 μl of DMSO. Wing buds from treated specimens were dissected 24 h later, and processed for EdU detection according to the manufacturer's protocol.

2.8. Statistics

In general, data are expressed as mean ± standard error of the mean (SEM). In qRT-PCR determinations, statistical analyses between groups were tested by the REST 2008 program (Relative Expression Software Tool V 2.0.7; Corbett Research) [31]. This program makes no assumptions about the distributions, evaluating the significance of the derived results by Pair-wise Fixed Reallocation Randomization Test tool in REST [31]. Statistical analyses of wing biometrical measurements were carried out with the Student's *t*-test.

3. Results

3.1. Broad-complex isoforms are expressed along the entire nymphal life of B. germanica

As a first step in our work, we studied the temporal expression of BR-C during the nymphal life of the cockroach *B. germanica*. Firstly, we used whole body extracts and a primer set amplifying a fragment in the core region of BR-C, which is common to the six BR-C isoforms. Results obtained show that BR-C transcripts are present in the six nymphal instars (N1 to N6) at levels of some 100 copies per 1000 copies of actin mRNA. In the last nymphal instar (N6), BR-C mRNA levels steadily decreased until becoming practically undetectable just before molting to the adult stage (Fig. 1A).

Given that BR-C functions in hemimetabolous insects appeared to be associated to wing growth, we obtained expression patterns in the pooled wing pads, that is, the lateral expansions of the mesonotum and metanotum, which contain the wing buds, during the last two nymphal instars (N5 and N6). Results revealed that BR-C is highly expressed in wing pads in N5, the expression levels forming a peak on day 4. In N6 the expression levels are notably lower and steadily decreasing, although showing a small peak of expression on day 6 (Fig. 1B). The expression peaks in N5 and N6 correspond to the peaks of 20E, and the high levels of expression in N5 correlate with the presence of JH, while the levels decrease in N6 when JH vanishes (Fig. 1B, bottom).

The expression of the individual isoforms, BR-C Z1 to BR-C Z6 in the wing pads during N6 shows the same pattern in all isoforms: high levels at emergence, then a steady decrease although with a small peak of expression on day 6 (Fig. 1C). Moreover, the study shows that BR-C Z2 is the most abundant isoform, followed by Z3, Z6, Z4, Z1 and Z5. With the RNA extract used to study the individual isoforms (results in Fig. 1C) we also amplified the core region fragment as in Fig. 1A. The mRNA values obtained were similar to those resulting from the sum of values of all isoforms for each day (Supplementary Fig. 1), which suggests that the six BR-C isoforms known in *B. germanica* constitute the complete functional set.

As stated above, the dramatic differences of BR-C expression between N5 and N6 are probably due to JH, which is abundantly present in N5 and practically absent in N6. This suggests that JH enhances the expression of BR-C in *B. germanica*, and that the decline of BR-C mRNA levels in N6 may largely be due to the absence of JH. In agreement with this, topical treatment of freshly emerged N6 with 20 μg of JH III induced the re-expression of BR-C (Fig. 1D). Congruently, depletion of Kr-h1, a transcription factor involved in early JH signaling, decreases BR-C expression levels in N4 and in N5 (Fig. 1E).

3.2. BR-C depletion impairs wing development

To study the role of BR-C, cockroaches were treated with 3 μg dsRNA targeting the core region of BR-C (dsBrCore) at day 0 of N5. The controls were equivalently treated with dsMock. On day 6 of N5 and on day 0 of N6, the levels of BR-C mRNA in dsBrCore-treated specimens were significantly lower than those measured in the controls (Fig. 2A). dsBrCore-treated specimens (n = 34) molted normally to N6, but the adults emerging from the subsequent molt showed a number of differences with respect to dsMock-treated controls (n = 24). In dsBrCore-treated specimens, both wing pairs were well extended, but the forewings appeared to be somewhat broader and the hindwings were smaller than those of the controls, and showed a number of vein defects (Fig. 2B). Biometrical data supported the observations regarding form and size (Supplementary Fig. 2). And as to the hind wing vein patterning, 19 out of 34 specimens (56%) had the CuP vein shorter and an associated notch at the wing edge (defect A, Supplementary Fig. 3); four specimens (12%) showed vein/intervein pattern disorganization in the anterior part of the wing (defect B, Supplementary Fig. 3); six specimens (17%) showed the defects A and B; and five specimens (15%) had A and B defects and their A-veins were subdivided and incomplete (defect C, Supplementary Fig. 3). In all other respects, the external morphology of the adult of dsBrCore-treated specimens was normal. Control (dsMock-treated) specimens developed normally patterned wings, although a small percentage of the specimens (3 out of 24, 12.5%) showed the defect B (Supplementary Fig. 3).

We then increased the RNAi effectiveness using two doses of 3 μg of dsBrCore, administered respectively on days 0 and 3 of N5. Levels of BR-C mRNA measured on day 6 of N5 (Fig. 2C) were lower than those obtained with a single injection (Fig. 2A). The specimens treated twice with dsBrCore (n = 23) molted normally to N6, and then to the adult stage, which showed malformed wings. About 70% of the adult specimens (16 out of 23) showed a phenotype similar to that obtained with a single injection of dsRNA: the wings being well extended but with the typical notch produced by a shortening of the CuP vein, a similar diversity of vein patterning malformations, and with broader forewings and smaller hindwings than in the controls (Fig. 2D, left). The remaining 30% exhibited a wing phenotype more severe, with the forewings and hindwings heavily reduced and so wrinkled (Fig. 2D, right) that it was difficult to extend them on a slide; however, close examination indicated that all of them had the A, B and C vein defects observed in the dsBrCore-treated specimens that emerged with the

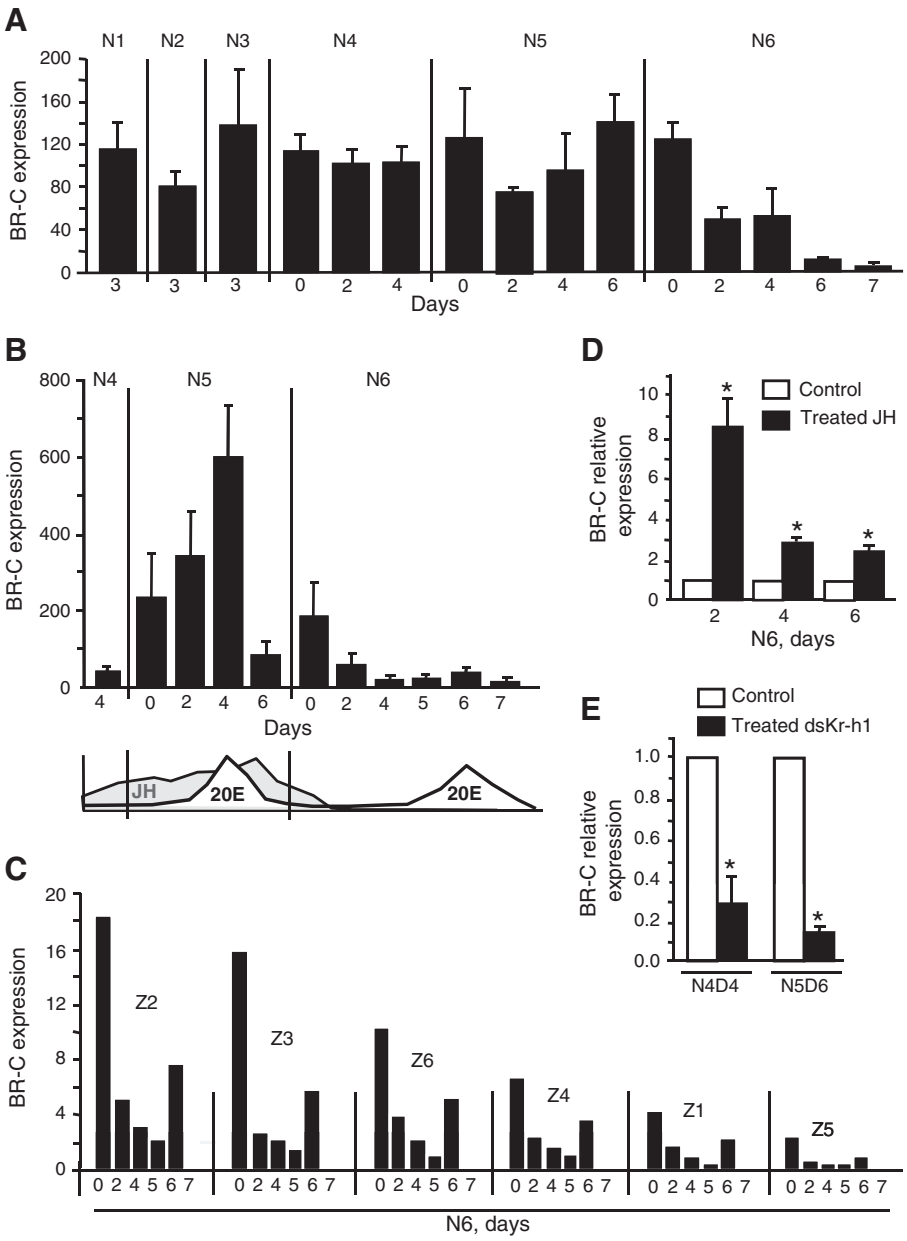

Fig. 1. Expression of BR-C mRNA in *Blattella germanica* female. (A) Joint expression of all isoforms in the whole body in selected days of the 6 nymphal instars: N1 to N6. (B) Joint expression of all isoforms in the mesonotum and metanotum wing pads in selected days of N4, N5 and N6. Concentration patterns of hemolymph juvenile hormone (JH) III and 20-hydroxyecdysone (20E) are indicated below, according to previously published data [33,40]. (C) Expression of individual BR-C isoforms (Z1 to Z6) in the wing pads on selected days of N6. (D) Effect of the application of 20 μg of JH III. The hormone was administered on freshly emerged N6 and BR-C mRNA levels were measured 2, 4 and 6 days later. (E) Effect of Kr-h1 depletion by RNAi on N4 and N5. Two doses (3 μg each) of dsKr-h1 (treated) or dsMock (control) were administered on N4 and N5 (on days 0 and 3 in both cases), and BR-C mRNA levels were measured on day 4 in the experiments of N4, and on day 6 in the experiments of N5. Data is represented as the mean ± SEM, and are indicated as copies of BR-C mRNA per 1000 copies of BgActin-5c. Each point represents 3–6 biological replicates, except in panel C, in which data represent one replicate per point. In panels D and E data are normalized against control females (arbitrary reference value = 1) and the asterisk indicates statistically significant differences with respect to controls ($p<0.05$), according to the REST software tool [31].

wings well extended. Arguably, differences in severity of the effects are due to differences of penetrance and intrinsic variability in these experiments. All the controls treated equivalently with two doses of dsMock (n = 18) emerged with normal wings in terms of size, form and vein patterning.

In order to assess whether BR-C could play a role on the wing development of younger instars, we administered two doses (3 μg-each) of dsBrCore on days 0 and 3 respectively of N4. On day 0 of N5, the levels of BR-C mRNA in dsBrCore-treated specimens were significantly lower than in the controls (dsMock-treated) (Fig. 2E). dsBrCore-treated specimens (n = 22) molted normally to N5 and to N6, but when molting to the adult stage they showed the wing malformations observed in the former experiments, with extended and wrinkled wing phenotypes, but with a higher proportion of the latter. Thus, only six out of 22 treated specimens (27%) showed the extended wing phenotype, and even these had the wings imperfectly extended (Fig. 2F, left); moreover, the wings exhibited the A, B and C defects and reduced size typical of BR-C knockdowns. The remaining 16 specimens (73%) showed the more severe wrinkled wing phenotype (Fig. 2F, right). The controls (dsMock-treated, n = 21), had normal wing patterning, except three specimens (14.3%) that exhibited the B defect.

Finally, we aimed at studying the effect of BR-C depletion in the last instar nymph (N6), where the transition to the adult stage occurs. Cockroaches were treated with two doses of 3 μg each of dsBrCore,

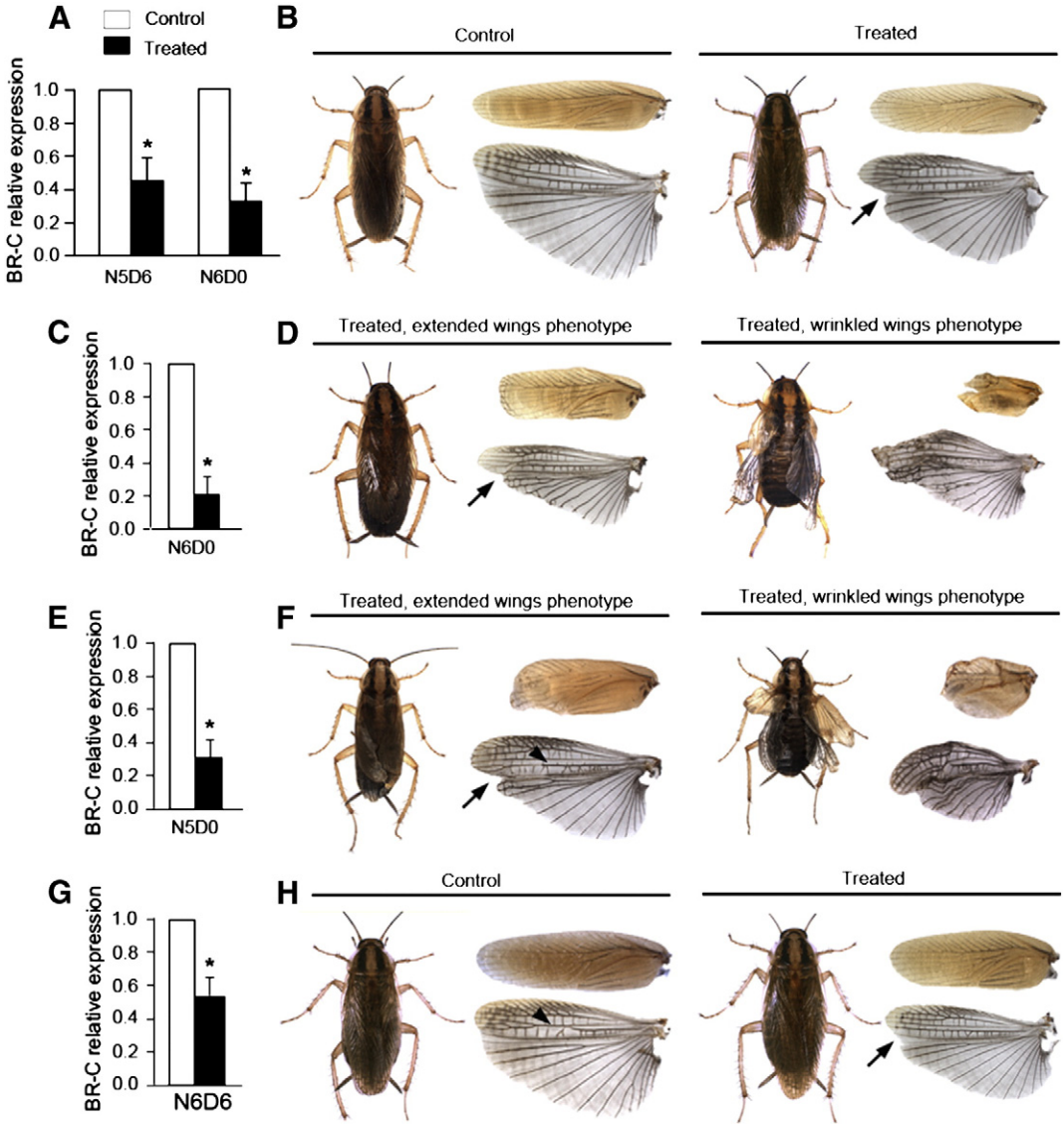

Fig. 2. Phenotype obtained after depleting all BR-C isoforms by RNAi in *Blattella germanica*. (A–B) Effect of a single 3 μg-dose of dsMock (control) or dsBR-core (treated) administered on day 0 of N5: BR-C mRNA levels on day 6 of N5 and on day 0 of N6 (A); adult phenotype (habitus, forewing and hindwing) (B). (C–D) Effects of two doses of 3 μg each of dsBR-core administered on day 0 and day 3 of N5: BR-C mRNA levels on day 0 of N6 (C); extended wings and wrinkled wings phenotype (D). (E–F) Effects of two 3 μg-doses of dsBR-core administered on day 0 and day 3 of N4: BR-C mRNA levels on day 0 of N5 (E); extended wings and wrinkled wings phenotype (F). (G–H) Effects of two 3 μg-doses of dsMock (control) or dsBR-core (treated) administered on day 0 and day 3 of N6: BR-C mRNA levels on day 6 of N6 (G); adult phenotype of controls and treated specimens (H). Data in (A), (C), (E) and (G) represent 3 biological replicates (mean ± SEM), are indicated as copies of BR-C mRNA per 1000 copies of BgActin-5c, and are normalized against control females (arbitrary reference value = 1); the asterisk indicates statistically significant differences with respect to controls ($p<0.05$), according to the REST software tool [31]. Arrows indicate the notch provoked by a shortening of the CuP vein, and the arrowhead indicates disorganized vein/intervein patterning in the anterior part of the hindwing. Note that the late defect appeared also in controls (H).

one administered on day 0 and the other on day 3 of N6. Three days later (day 6), the levels of BR-C mRNA were significantly lower in dsBrCore-treated insects than in the controls (Fig. 2G). All adults obtained after this treatment (n = 24) emerged with the wings well extended, and only 5 of them (21%) showed the A defect (Fig. 2H, right). Control (dsMock-treated) specimens (n = 23) had normal wing patterning, and only one specimen (4%) had the B defect (Fig. 2H, left).

3.3. BR-C depletion impairs cell division in wing buds

The decrease in wing size, especially in the hindwings, suggests that there was a problem of cell proliferation in dsBrCore-treated specimens. To test this possibility, we first studied cell division in the hindwing buds in N6 around the peak of 20E, which takes place between days 5 and 7, with maximum values on day 6 [40]. Cell division in the hindwing buds, which are located within a pocket in the lateral expansions of the metanotum, was labeled with EdU. On day 5, EdU labeling revealed intense cell division on the surface of the hindwing bud (Fig. 3A, day 5). On day 6, cell division on the surface practically vanished, while the wing bud started growing and folding (Fig. 3A, day 6). Towards the end of day 6 and during the whole of day 7, EdU labeling disappeared and a remarkable, general wing growth took place, that provoked multiple and thick folds on the hindwing surface (Fig. 3A, day 7). The same transition from cell division to wing growth between days 5 and 7 occurs in the forewing buds (Fig. 3B, control), which are located within the lateral expansions of the mesonotum.

In specimens treated with a double dose of 3 μg of dsBrCore administered respectively on days 0 and 3 of N5, EdU labeling in the forewing buds on day 5 of N6 was significantly reduced in comparison with

controls (dsMock-treated) (Fig. 3B, left panels, compare the control and the treated). On day 6, during the period of growth and folding in controls, remarkable surface reduction was noticed along the edges of the wing pad in dsBrCore-treated specimens (Fig. 3B, right panels, compare the control and the treated), which parallels the statistically significant reduction on wing size measured after the imaginal molt (Supplementary Fig. 2). Concerning the hindwing buds, EdU labeling on day 5 was also more reduced in the specimens treated with dsBrCore than in controls treated with dsMock. Differences were particularly obvious at the distal end of the CuP vein, were EdU labeling was practically absent in dsBrCore-treated specimens, in comparison with the controls (Fig. 3C). Interestingly, the distal end of the CuP vein, where there is no cell division, disappeared thereafter, on day 6, at the maximum peak of ecdysone, therefore forming the characteristic notch of the BR-C knockdowns (Fig. 2B, D, F, H and Supplementary Fig. 3). In the subsequent stage of tissue growth without cell division, from the end of day 6 to the ecdysis, on day 8, differences between dsBrCore-treated specimens and controls were not apparent in either the forewing bud or the hindwing bud. We also used EdU labeling to study wing bud cell division around the 20E peak of N5 in specimens that had been treated with two doses of dsBrCore on days 0 and 3 of N4. Results showed that cell division was lower in dsBRCore-treated specimens than in controls (dsMock-treated), both in the forewing and in the hindwing buds (results not shown), as occurred in N6.

3.4. Functions of individual BR-C isoforms in B. germanica

All BR-C isoforms, from Z1 to Z6, are expressed simultaneously, although at different levels, and show the same pattern (Fig. 1C), suggesting that all of them contribute to the same functions in post-embryonic development. However, we aimed to test this conjecture by carrying out isoform-specific RNAi experiments on all isoforms. Treatments were carried out in N5, by injecting two doses of 3 μg of the corresponding BR-C dsRNA (dsBrZ1 to dsBrZ6), one on day 0 and the other on day 3. The controls were equivalently treated with dsMock.

Transcript depletion of the specifically targeted isoform was measured on the wing pads on day 0 of N6. Transcript levels of all other non-targeted isoforms were also measured as a control of RNAi specificity. Results (Fig. 4A–F) show that, in general, individual isoform RNAi experiments were isoform-specific in terms of transcript depletion. Treatment with dsBrZ3 reduced BR-C Z3 mRNA levels, but differences with respect to the corresponding controls were not statistically significant. This treatment also tended to reduce BR-C Z2 mRNA levels and, intriguingly, tended to increase the mRNA levels of BR-C Z4, BR-C Z5 and BR-C Z6 (Fig. 4B). It is also worth noting that treatment with dsBrZ4 significantly reduced BR-C Z4 mRNA levels, as expected, but also those of BR-C-Z5 (Fig. 4D).

In terms of phenotype, all specimens in all isoform-specific RNAi experiments molted normally to N6 and then to adult. A detailed examination of the external morphology of the adult was then performed and differences with respect to controls were only noticed in the wings of specimens treated with dsBrZ2 and dsBrZ6. Concerning dsBrZ2-treated specimens (n = 27), 18 of them (67%) had only the A defect (Fig. 4G); 1 (4%) showed only the B defect; and 7 (26%) had no visible defects. No significant differences were observed in wing sizes between treated specimens and controls, neither in the hindwing nor in the forewing. The hindwing phenotype resembles that obtained when depleting all isoforms simultaneously, but less marked, with less penetrance and without the C defect (see Supplementary Fig. 3). All control (dsMock-treated) specimens (n = 12) showed normal wing patterning except one specimen (8%) that had the B defect. In the dsBrZ6-treated group (n = 25), 9 specimens (36%) showed the B defect (Fig. 4H), whereas the remaining 16 were perfectly patterned. In the control group (dsMock-treated) (n = 18), 2 specimens (11%) showed the B defect.

Specimens obtained from RNAi experiments targeting Z1 (dsBrZ1-treated, n = 18; dsMock-treated, n = 10), Z3 (dsBrZ3-treated, n = 24; dsMock-treated, n = 14), Z4 (dsBrZ4-treated, n = 16; dsMock-treated, n = 11) and Z5 (dsBrZ5-treated, n = 18; dsMock-treated, N = 10), had the wings well extended and correctly patterned (Fig. 4I), and only a

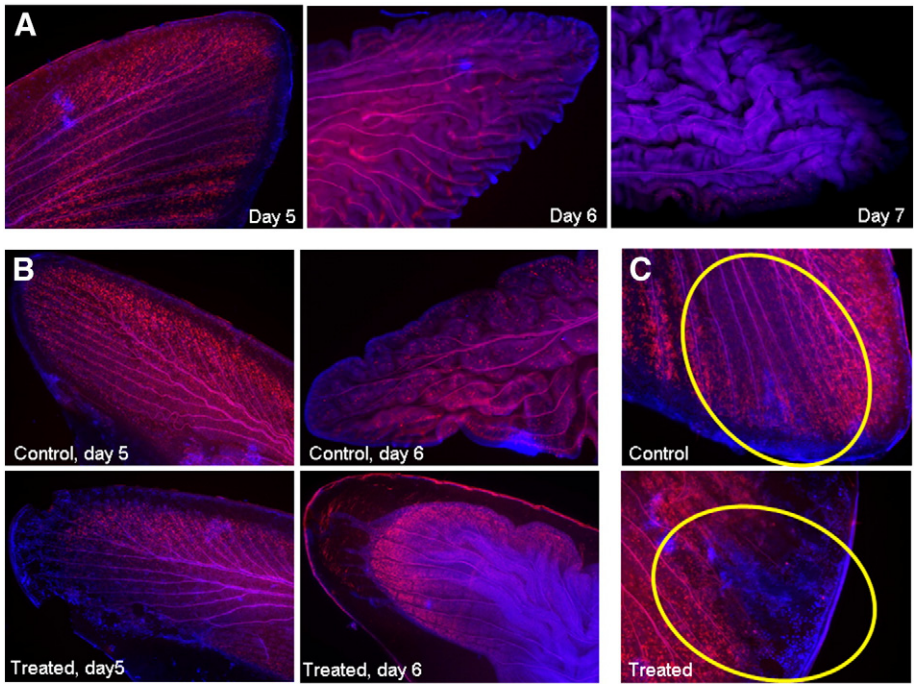

Fig. 3. Development of wing buds in control and BR-C knockdown specimens of *Blattella germanica*. (A) Double labeling EdU (discrete red spots) and DAPI (blue color) of a hindwing bud of untreated females on days 5, 6 and 7 of the last nymphal instar (N6). (B) EdU-DAPI double labeling of a forewing bud of females that were treated with two doses of dsBrCore (treated) or of dsMock (control) administered on days 0 and 3 of N5, and photographed on days 5 and 6 of N6. (C) EdU-DAPI double labeling of a hindwing bud of females that were treated as in (B) and photographed on day 5 of N6; the pictures show the region corresponding to the distal end of the CuP vein (yellow oval).

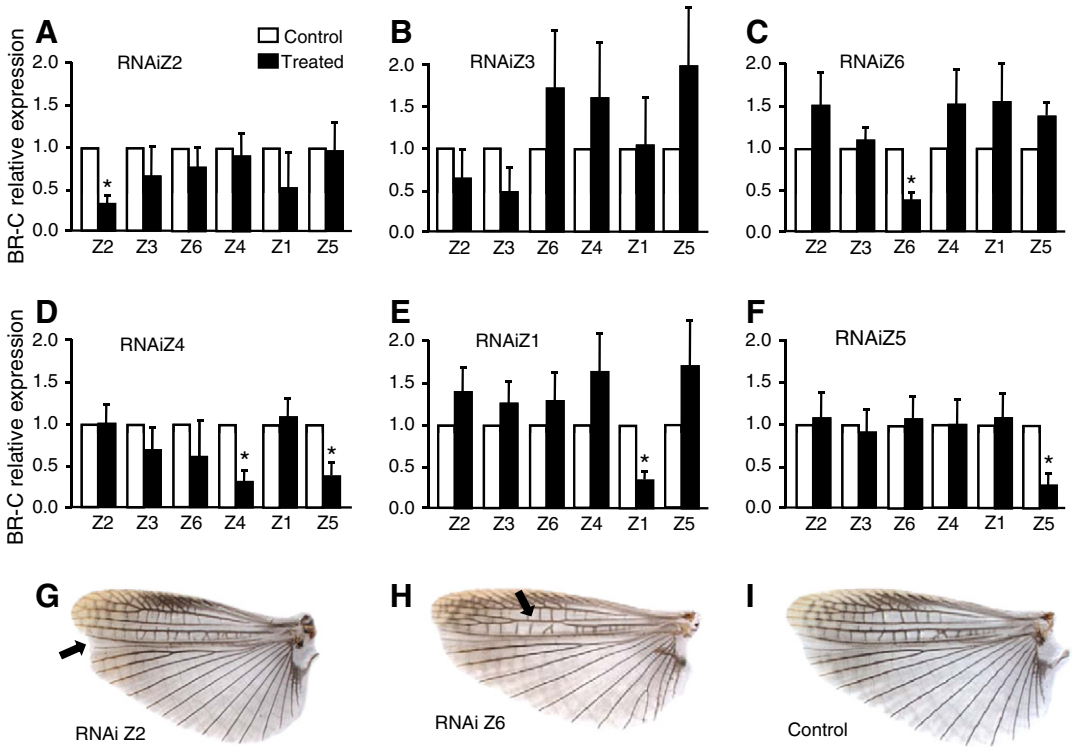

Fig. 4. Effects obtained after depleting each BR-C isoform, from Z1 to Z6, individually, by RNAi in *Blattella germanica*. (A–F) Transcript levels of the targeted and the other isoforms measured in the mesonotum and metanotum wing pads on the day 0 of N6. Two 3-μg doses of dsBrZ2 (A), dsBrZ3 (B), dsBrZ6 (C), dsBrZ4 (D), dsBrZ1 (E) or dsBrZ5 (F) administered on days 0 and 3 of N5; control received an equivalent treatment with dsMock; data represent 3 biological replicates (mean ± SEM) and are indicated as copies of the individual BR-C isoforms mRNA per 1000 copies of BgActin-5c; the asterisk indicates statistically significant differences with respect to controls ($p<0.05$), according to the REST software tool [31]. (G–I) Adult hindwing phenotype studied 3 days after the imaginal molt, from a dsBrZ2-treated specimen (G), a dsBrZ6-treated specimen (H), and from a control specimen treated with dsMock. The arrow indicates the main defects: the notch at the end of the CuP vein in G and the vein pattern disorganized in the anterior part of the wing in H.

few specimens (between 0 and 14%, irrespective of the group, either in the treated or the control) had the B defect.

4. Discussion

4.1. The patterns and the hormonal environment

In *B. germanica*, BR-C isoforms are expressed in all nymphal stages, and expression only declines in the last, pre-imaginal stage. The expression pattern is similar in all individual isoforms of BR-C, although the respective abundances differ, Z2 being the most abundant, followed by Z3, Z6, Z4, Z1 and Z5. Expression is more intense in the wing pads, and the pattern appears to be determined by the hormonal environment: maximum BR-C mRNA levels coincide with bursts of 20E production in the presence of high levels of JH. The coincidence of BR-C expression peaks and those of 20E reflects cause–effect relationships, as expression of BR-C is 20E-dependent [41]. Then, BR-C mRNA levels decline in the last nymphal instar (N6), in parallel to JH vanishing, although a small burst of expression is still observed on day 6 coinciding with a peak of 20E. The correspondence of BR-C and JH patterns, the induction of BR-C expression by exogenous JH III, and their down-regulation after depletion of Kr-h1, suggest that JH enhances BR-C expression during young nymphal instars. Therefore, the steady decline observed in N6 must be due, at least in part, to the decrease of JH titer. In the hemipteran *P. apterus*, treatment with a JH analogue induces ectopic expression of BR-C in last nymphal instar, whereas depletion of Met expression led to a significant reduction of BR-C expression [12]. These observations are in agreement with our present results as Met is an early transducer of the JH signal and seems to play a role in JH reception [9], also in *B. germanica* (our unpublished results).

Significant expression of BR-C in young nymphal instars has been reported in the hemimetabolous species *O. fasciatus* [29] and *P. apterus* [12]. Conversely, BR-C expression in holometabolous species is quantitatively relevant only in the larva–pupa transition. This includes *D. melanogaster* [25], *M. sexta* [25], *B. mori* [42] and *T. castaneum* [11,27,28]. Data from holometabolous species suggest that the onset of BR-C expression occurs after a small burst of 20E produced in the absence of JH at the end of the last larval instar. In *M. sexta*, BR-C transcripts appear at the end of the feeding stage (beginning of wandering behavior) in the epidermis of the last instar larvae, when the insect becomes committed to pupal differentiation. Administration of JH in this stage prevents the 20E-induced expression of BR-C [43]. Later, levels of BR-C mRNA decrease during the pupal stage and the pupae transform into the adult stage. In the pupae, exogenous JH induces the re-expression of BR-C, and the insect undergoes a second pupal molt [25].

The expression patterns of BR-C isoforms in the thysanopterans *Frankliniella occidentalis* and *Haplothrips brevitubus* [44], are especially interesting. Thysanopterans follow an essentially hemimetabolous development, in the sense that nymphs are morphologically similar to adults, but the life cycle includes 1 to 3 quiescent stages, called propupae and pupae, where wing buds develop considerably and which are reminiscent of the holometabolous pupal stage. This particular cycle has been distinguished as neometabolan development [5]. *F. occidentalis* has two nymphal stages, a propupal and a pupal stage, whereas *H. brevitubus* has two nymphal stages, a propupal and two pupal stages. In both species, expression of BR-C is low in the first instar nymph, peaks towards the end of the second instar nymph and decreases in the propupae. Moreover, treatment of propupae with a JH analogue induces the re-expression of BR-C in the pupae [44]. The BR-C expression pattern, showing a peak just before the transition from nymph to propupae, and the stimulatory effect of JH on BR-C expression in the

propupae, are reminiscent of the endocrine determinism of the pupal stage in holometabolous species.

4.2. The functions

RNAi experiments in nymphs of *B. germanica* have shown that wing buds experience intense cell proliferation, which is hampered in BR-C knockdowns. This suggests that BR-C isoforms regulate progressive growth of wing buds during nymphal life by promoting cell division. In the last nymphal instar there is a phase of cell proliferation encompassed by the increasing levels of 20E that lead to the peak on day 6, followed by a phase of cell growth and wing metamorphosis encompassed by the decreasing levels of 20E that occur after the peak. In this metamorphic instar, cell proliferation is also hampered in BR-C knockdowns, but the subsequent phase of cell growth and metamorphosis is generally not affected by BR-C RNAi. Only some details of vein patterning in the hindwing are affected by BR-C RNAi, including the length of the CuP vein, the organization of the longitudinal and small transversal veins in the anterior part of the hindwing, and the linear growth of the A-veins in the posterior part.

Therefore, the function of BR-C isoforms in postembryonic development of *B. germanica* appears to be restricted to sustaining cell division in the wing buds, which contributes to the final size and morphology of the adult wings, and regulation of a number of details of vein patterning and length and in the hindwing. While the latter function had not been described before in hemimetabolous insects, our observations on wing size are equivalent to those obtained in *O. fasciatus* and *P. apterus*, where RNAi treatments of BR-C hampered wing bud development in nymphs and resulted in adults with reduced and wrinkled wings [12,29]. Our observations refer to the external morphology, as no anatomical examinations were carried out during the present work. Thus, we cannot rule out the possibility of a possible role of BR-C factors in the nervous system during metamorphosis of *B. germanica*, as what occurred in *D. melanogaster* [45,46]. However, the primitive hemimetaboly exhibited by *B. germanica* suggests that there are no dramatic transformations of the internal organs, as opposed to *D. melanogaster*, whose internal anatomy is heavily reconstructed during metamorphosis.

In striking contrast, BR-C proteins play complex morphogenetic roles in holometabolous species, leading to the formation of the pupal morphology. Pioneering genetic studies in *D. melanogaster* demonstrated that BR-C null mutants, in which not one of the isoforms is expressed, never molt to pupae [23,47,48]. Later, the use of a recombinant Sindbis virus expressing a BR-C antisense RNA fragment in *B. mori* reduced endogenous BR-C mRNA levels in infected tissues and the insect did not complete the larval–pupal transition [26]. More recently, experiments depleting BR-C mRNA levels with RNAi have been carried out in *T. castaneum* [11,27,28] and in the lacewing *Chrysopa perla* [28]. In all cases, RNAi treatments in larvae hampered larval–pupal transformation and produced individuals with larval, pupal and adult features, which indicates that BR-C isoforms promote the pupal developmental program while suppressing those of the larvae and the adult.

4.3. The isoforms

In *D. melanogaster*, BR-C encodes four zinc-finger protein isoforms (Z1, Z2, Z3 and Z4), which share most of the amino-terminal region called the BRcore, but they have a unique pair of zinc-fingers at their carboxy terminus [23,24]. Moreover, the common BRcore region contains a BR-C-Tramtrack-Bric-à-brac (BTB) domain involved in protein–protein interactions [24]. Mutants corresponding to isoform-specific regions form three complementing groups: *br* (broad), *rbp* (reduced bristle number on palpus) and *2Bc* [47,48]. Alleles belonging to the *npr1* (nonpupariating1) class of mutations do not complement mutations in each of the three complementing genetic functions. *npr1* mutations result in developmental arrest and lethality at pupariation; br^+ function is required for wing and leg imaginal disc development and for tanning the larval cuticle; rbp^+ and $2Bc^+$ functions are needed for larval tissues destruction and for gut morphogenesis; moreover, $2Bc^+$ is additionally required for complete closure of the thoracic epidermis, and all three functions must occur for central nervous system reorganization [47–50]. Mutant rescue experiments associated protein isoforms with genetic functions, and revealed that there were isoform-specific functions, although with some degree of redundancy [51]. Further studies in *D. melanogaster* have shown specific space–temporal distributions of different BR-C isoforms, thus suggesting distinct temporal function, especially in neural tissue morphogenesis [45,46,52]. Finally, the advent of RNAi allowed the functional study of individual BR-C isoforms (Z1 to Z5) in *T. castaneum* metamorphosis. As in *D. melanogaster*, results pointed to isoform-specific roles and partial redundancy [27,28].

Our functional studies on specific isoforms revealed that depletion of BR-C Z2 and BR-C Z6 gave discernible phenotypes, in both cases related to wing patterning. BR-C Z2 phenotype showed the CuP vein shorter and an associated notch at the wing edge (defect A), and the vein/intervein patterning disorganized in the anterior part (defect B), but it did not show the A-veins subdivided and incomplete (defect C). Moreover, the penetrance and severity of the defects were lower in comparison with the BR-C Core knockdowns, while wing size was practically unaffected. BR-C Z6 knockdowns phenotype showed t defects B and C, but not defect A, which is the most typical in the experiments depleting all isoforms simultaneously; wing size was unaffected. Phenotypes obtained in RNAi experiments on BR-C Z1, BR-C Z3, BR-C Z4 and BR-C Z5 were as in controls, including defect B, which seems qualitatively unspecific, although, importantly, its occurrence in BRCore or BR-C Z6 knockdowns is significantly higher than in controls. The relatively poor abundance of these isoforms in the pool of BR-C proteins, and the generally modest efficiency of these RNAi experiments in terms of transcript decrease, might explain the absence of differential phenotypes. However, given that phenotypes observed in BR-C Z2 and BR-C Z6 knockdowns encompass all the defects observed in BRCore knockdowns, we can presume that functions of the remaining isoforms might be redundant with those of BR-C Z2 and BR-C Z6.

4.4. Conclusion: the evolution of metamorphosis at the light of BR-C

The main function played by BR-C proteins in *B. germanica*, a phylogenetically basal, hemimetabolous species, during post-embryogenesis is to promote wing growth to reach the right size and form. Basically, this function has been conserved in the hemimetabolous species *O. fasciatus* and *P. apterus*, which are phylogenetically more distal than *B. germanica*. In these bugs, the wing buds are external, not embedded in a cuticular wing pad pocket, and the decrease in growth and attenuation of color pattern progression of BR-C knockdowns is externally visible [12,29]. In the beetle *T. castaneum*, RNAi of BR-C isoforms Z2 and Z3 results in pupae with shortened wings [27], which indicates that functions of BR-C related to wing size are conserved in basal holometabolous species. Functions of BR-C in determining wing size and form also appear to be present in the extremely modified, holometabolous species of fly *D. melanogaster*. Indeed, the name “broad” given to one of the complementation groups of BR-C derives from the oval, rather than from the elliptic form of the wings of these mutants, which were first described by Thomas H. Morgan and colleagues in 1925 [53]. Therefore, the functions of BR-C related to controlling wing size and form appear to be ancestral and conserved from cockroaches to flies. The same may hold true for the subtle functions related to vein patterning observed in *B. germanica*, as the classical *br* mutants of *D. melanogaster* also have defects on vein length [53]. Vein patterning in BR-C knockdowns of *O. fasciatus* and *P. apterus* was not reported [12,29].

Another interesting feature of BR-C in *B. germanica* is that its expression is enhanced by JH. Thus, both JH and BR-C mRNA levels are high in young nymphal instars and decrease in parallel during

the last nymphal instar, prior to metamorphosis. This contrasts with the situation found in holometabolous species, where JH inhibits BR-C expression in young larvae, and so high levels of JH correlate with low levels of BR-C expression [12].

A number of theories have been proposed to explain the evolutionary transition from hemimetaboly to holometaboly [4,54]. A classic theory originally argued by Lubbock [55] and formalized by Berlese [56], proposes that the larvae of holometabolous species arose by "de-embryonization", so that it was a sort of free living, often vermiform embryo. The "de-embryonization" theory was resuscitated and reinforced with modern endocrine data by Truman and Riddiford [54], who proposed that the holometabolous larva corresponds to the latest hemimetabolous embryonic stage that the latter authors called the pronymph, and that the origin of larval form would be explained by a shift in JH titers, from late embryonic stages in hemimetabolous species to earlier stages in holometabolous insect embryos. Thus, in postembryonic stages of holometabolous species, only when JH declines in the final larval instar does extensive morphogenesis resume and lead to differentiation of the pupa [57].

While this theory still is under debate [4], our present results show that, in a basal hemimetabolous species, JH enhances the expression of BR-C in young nymphs and that BR-C factors promote wing growth during nymphal life and refine wing patterning at metamorphosis, which contrasts with the endocrine regulation and complex functions observed in holometabolous species, as previously described in classical insect models. We propose that in the evolution from hemimetaboly to holometaboly, at least two key innovations appeared that affected BR-C and post-embryonic morphological development. The first was a shift of JH action, from stimulatory (as in present hemimetabolous species) to inhibitory (present holometabolous species) of BR-C expression, during young stages. Thus, BR-C expression had become inhibited during young larvae in holometabolous ancestors, with the resulting suppression of growth and development of BR-C-dependent tissues, for example the wing bud. The second great innovation was an expansion of functions, from one specialized in wing development and details of vein patterning, as in present hemimetabolous species, to a larger array of morphogenetic functions, which culminated with the pupal-specifier role that operates in present holometabolous species, from the basal *T. castaneum* to the distal *D. melanogaster* (Fig. 5). Paradoxically, the number of isoforms decreased from six to four in the evolution from cockroaches to flies, while their functions dramatically expanded.

The case of thysanopterans is very interesting because they show the so-called neometabolous development [5], with a life cycle including quiescent "propupal" and "pupal" stages that are reminiscent of the holometabolous pupae. The studies in *F. occidentalis* and *H. brevitubus* of Minakuchi et al. [44] have shown that BR-C mRNA levels are very low in young instars and show an acute peak around the formation of the propupae, as what occurred in holometabolous species, suggesting that BR-C expression in thysanopterans is hormonally regulated and specified as in holometabolous species. Reconstructions of insect phylogeny suggest that paraneopterans ((thysanopterans + hemipterans) + (psocopterans and phthirapterans)) are the sister group of holometabola [58]. If so, then the first steps towards the innovation of the pupal stage, including the endocrine determination, might have occurred in the ancestor of paraneoptera + holometabola. Interestingly, hemipterans also contain representatives of neometabolous development in the sternorrhyncha [4,5]. Our hypothesis contemplates that other hemipterans, and psocopterans and phthirapterans would have lost the ability to produce preimaginal quiescent stages in their life cycles. Whichever the case, although natural selection was able to make a first attempt to invent a sort of pupa in the ancestor of the paraneoptera + holometabola, the invention was fully perfected in the lineage of holometabola judging by the endless forms most beautiful that stand today in this insect superorder.

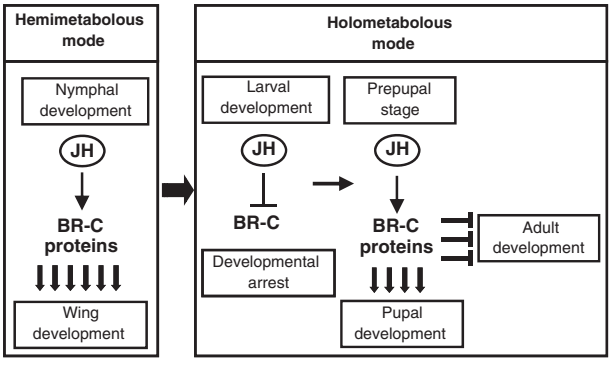

Fig. 5. BR-C and the evolution of insect metamorphosis. In the transition from hemimetaboly to holometaboly, the regulation and functions of BR-C would have experienced two main changes. First, a shift of JH action on BR-C expression, from stimulatory in hemimetabolous to inhibitory in holometabolous species. Second, an expansion of functions, from controlling wing pad growth by cell proliferation along nymphal instars, and regulating subtle features of vein development and patterning (hemimetabolous), to regulating pupal formation and inhibiting adult features at the end of the larval life (holometabolous).

Acknowledgement

Financial support for this research was provided by the Spanish MICINN (grant CGL2008-03517/BOS to X.B. and predoctoral fellowship to J.L.) and by the CSIC (grant 2010TW0019, from the Formosa program, to X.B.). J.-H.H. received a grant from the National Research Council (Taiwan) to work in the Institute of Evolutionary Biology, in Barcelona. Thanks are also due to Maria-Dolors Piulachs for helpful discussions, and to José Martínez for helping in the experimental work.

Appendix A. Supplementary data

Supplementary data to this article can be found online at http://dx.doi.org/10.1016/j.bbagen.2012.09.025.

References

[1] C. Darwin, The Origin of Species by Means of Natural Selection, or the Preservation of Favoured Races in the Struggle for Life, John Murray, London, 1872.
[2] D. Grimaldi, M.S. Engel, Evolution of the Insects, Cambridge University Press, Cambridge, 2005.
[3] P. Hammond, Species inventory, in: B. Groombridge (Ed.), Global Biodiversity, Chapman and Hall, London, 1992, pp. 17–39.
[4] X. Belles, Origin and evolution of insect metamorphosis, in: Encyclopedy of Life Sciences, John Wiley and Sons, Ltd., Chichester, 2011.
[5] F. Sehnal, P. Svacha, J. Zrzavy, Evolution of insect metamorphosis, in: L.I. Gilbert, J.R. Tata, B.G. Atkinson (Eds.), Metamorphosis, Academic Press, San Diego, 1996, pp. 3–58.
[6] J.W. Truman, L.M. Riddiford, Endocrine insights into the evolution of metamorphosis in insects, Annu. Rev. Entomol. 47 (2002) 467–500.
[7] L.M. Riddiford, How does juvenile hormone control insect metamorphosis and reproduction?, Gen. Comp. Endocrinol. (in press), http://dx.doi.org/10.1016/j.ygcen.2012.06.001.
[8] M. Jindra, S.R. Palli, L.M. Riddiford, The Juvenile Hormone Signaling Pathway in Insect Development, Annu. Rev. Entomol. (in press), http://dx.doi.org/10.1146/annurev-ento-120811-153700.
[9] J.P. Charles, T. Iwema, V.C. Epa, K. Takaki, J. Rynes, M. Jindra, Ligand-binding properties of a juvenile hormone receptor, Methoprene-tolerant, Proc. Natl. Acad. Sci. U. S. A. 108 (2011) 21128–21133.
[10] B. Konopova, M. Jindra, Juvenile hormone resistance gene Methoprene-tolerant controls entry into metamorphosis in the beetle *Tribolium castaneum*, Proc. Natl. Acad. Sci. U. S. A. 104 (2007) 10488–10493.
[11] R. Parthasarathy, A. Tan, H. Bai, S.R. Palli, Transcription factor broad suppresses precocious development of adult structures during larval–pupal metamorphosis in the red flour beetle, *Tribolium castaneum*, Mech. Dev. 125 (2008) 299–313.
[12] B. Konopova, V. Smykal, M. Jindra, Common and distinct roles of juvenile hormone signaling genes in metamorphosis of holometabolous and hemimetabolous insects, PLoS One 6 (2011) e28728.
[13] C. Minakuchi, X. Zhou, L.M. Riddiford, Krüppel homolog 1 (Kr-h1) mediates juvenile hormone action during metamorphosis of *Drosophila melanogaster*, Mech. Dev. 125 (2008) 91–105.
[14] C. Minakuchi, T. Namiki, T. Shinoda, Krüppel homolog 1, an early juvenile hormone-response gene downstream of Methoprene-tolerant, mediates its

anti-metamorphic action in the red flour beetle *Tribolium castaneum*, Dev. Biol. 325 (2009) 341–350.
[15] J. Lozano, X. Belles, Conserved repressive function of Krüppel homolog 1 on insect metamorphosis in hemimetabolous and holometabolous species, Sci. Rep. 1 (2011) 163.
[16] K. King-Jones, C.S. Thummel, Nuclear receptors—a perspective from *Drosophila*, Nat. Rev. Genet. 6 (2005) 311–323.
[17] Y. Nakagawa, V.C. Henrich, Arthropod nuclear receptors and their role in molting, FEBS J. 276 (2009) 6128–6157.
[18] C.S. Thummel, Ecdysone-regulated puff genes 2000, Insect Biochem. Mol. Biol. 32 (2002) 113–120.
[19] V.P. Yin, C.S. Thummel, Mechanisms of steroid-triggered programmed cell death in *Drosophila*, Semin. Cell Dev. Biol. 16 (2005) 237–243.
[20] J. Cruz, C. Nieva, D. Mane-Padros, D. Martin, X. Belles, Nuclear receptor BgFTZ-F1 regulates molting and the timing of ecdysteroid production during nymphal development in the hemimetabolous insect *Blattella germanica*, Dev. Dyn. 237 (2008) 3179–3191.
[21] D. Mane-Padros, F. Borras-Castells, X. Belles, D. Martin, Nuclear receptor HR4 plays an essential role in the ecdysteroid-triggered gene cascade in the development of the hemimetabolous insect *Blattella germanica*, Mol. Cell. Endocrinol. 348 (2012) 322–330.
[22] D. Martin, O. Maestro, J. Cruz, D. Mane-Padros, X. Belles, RNAi studies reveal a conserved role for RXR in molting in the cockroach *Blattella germanica*, J. Insect Physiol. 52 (2006) 410–416.
[23] C.A. Bayer, B. Holley, J.W. Fristrom, A switch in Broad-Complex zinc-finger isoform expression is regulated posttranscriptionally during the metamorphosis of *Drosophila* imaginal discs, Dev. Biol. 177 (1996) 1–14.
[24] P.R. DiBello, D.A. Withers, C.A. Bayer, J.W. Fristrom, G.M. Guild, The *Drosophila* Broad-Complex encodes a family of related proteins containing zinc fingers, Genetics 129 (1991) 385–397.
[25] X. Zhou, L.M. Riddiford, Broad specifies pupal development and mediates the 'status quo' action of juvenile hormone on the pupal–adult transformation in *Drosophila* and *Manduca*, Development 129 (2002) 2259–2269.
[26] M. Uhlirova, B.D. Foy, B.J. Beaty, K.E. Olson, L.M. Riddiford, M. Jindra, Use of Sindbis virus-mediated RNA interference to demonstrate a conserved role of Broad-Complex in insect metamorphosis, Proc. Natl. Acad. Sci. U. S. A. 100 (2003) 15607–15612.
[27] Y. Suzuki, J.W. Truman, L.M. Riddiford, The role of Broad in the development of *Tribolium castaneum*: implications for the evolution of the holometabolous insect pupa, Development 135 (2008) 569–577.
[28] B. Konopova, M. Jindra, Broad-Complex acts downstream of Met in juvenile hormone signaling to coordinate primitive holometabolan metamorphosis, Development 135 (2008) 559–568.
[29] D.F. Erezyilmaz, L.M. Riddiford, J.W. Truman, The pupal specifier broad directs progressive morphogenesis in a direct-developing insect, Proc. Natl. Acad. Sci. U. S. A. 103 (2006) 6925–6930.
[30] M.D. Piulachs, V. Pagone, X. Belles, Key roles of the Broad-Complex gene in insect embryogenesis, Insect Biochem. Mol. Biol. 40 (2010) 468–475.
[31] M.W. Pfaffl, G.W. Horgan, L. Dempfle, Relative expression software tool (REST) for group-wise comparison and statistical analysis of relative expression results in real-time PCR, Nucleic Acids Res. 30 (2002) e36.
[32] F. Camps, J. Casas, F.J. Sanchez, A. Messeguer, Identification of juvenile hormone III in the hemolymph of *Blattella germanica* adult females by gas chromatography–mass spectrometry, Arch. Insect Biochem. Physiol. 6 (1987) 181–189.
[33] K. Treiblmayr, N. Pascual, M.D. Piulachs, T. Keller, X. Belles, Juvenile hormone titer versus juvenile hormone synthesis in female nymphs and adults of the German cockroach, *Blattella germanica*, J. Insect Sci. 6 (2006) 47.
[34] E. Gomez-Orte, X. Belles, MicroRNA-dependent metamorphosis in hemimetabolan insects, Proc. Natl. Acad. Sci. U. S. A. 106 (2009) 21678–21682.
[35] X. Belles, Beyond *Drosophila*: RNAi in vivo and functional genomics in insects, Annu. Rev. Entomol. 55 (2010) 111–128.
[36] L. Ciudad, M.D. Piulachs, X. Belles, Systemic RNAi of the cockroach vitellogenin receptor results in a phenotype similar to that of the *Drosophila* yolkless mutant, FEBS J. 273 (2006) 325–335.
[37] J.L. Maestro, X. Belles, Silencing allatostatin expression using double-stranded RNA targeted to preproallatostatin mRNA in the German cockroach, Arch. Insect Biochem. Physiol. 62 (2006) 73–79.
[38] A. Salic, T.J. Mitchison, A chemical method for fast and sensitive detection of DNA synthesis in vivo, Proc. Natl. Acad. Sci. U. S. A. 105 (2008) 2415–2420.
[39] F. Chehrehasa, A.C. Meedeniya, P. Dwyer, G. Abrahamsen, A. Mackay-Sim, EdU, a new thymidine analogue for labelling proliferating cells in the nervous system, J. Neurosci. Methods 177 (2009) 122–130.
[40] I. Romaña, N. Pascual, X. Bellés, The ovary is a source of circulating ecdysteroids in *Blattella germanica* (L.) (Dictyoptera, Blattellidae), Eur. J. Entomol. 92 (1995) 93–103.
[41] F.D. Karim, G.M. Guild, C.S. Thummel, The *Drosophila* Broad-Complex plays a key role in controlling ecdysone-regulated gene expression at the onset of metamorphosis, Development 118 (1993) 977–988.
[42] A.M. Reza, Y. Kanamori, T. Shinoda, S. Shimura, K. Mita, Y. Nakahara, M. Kiuchi, M. Kamimura, Hormonal control of a metamorphosis-specific transcriptional factor Broad-Complex in silkworm, Comp. Biochem. Physiol. B Biochem. Mol. Biol. 139 (2004) 753–761.
[43] B. Zhou, K. Hiruma, T. Shinoda, L.M. Riddiford, Juvenile hormone prevents ecdysteroid-induced expression of broad complex RNAs in the epidermis of the tobacco hornworm, *Manduca sexta*, Dev. Biol. 203 (1998) 233–244.
[44] C. Minakuchi, M. Tanaka, K. Miura, T. Tanaka, Developmental profile and hormonal regulation of the transcription factors broad and Krüppel homolog 1 in hemimetabolous thrips, Insect Biochem. Mol. Biol. 41 (2011) 125–134.
[45] R.F. Spokony, L.L. Restifo, Broad Complex isoforms have unique distributions during central nervous system metamorphosis in *Drosophila melanogaster*, J. Comp. Neurol. 517 (2009) 15–36.
[46] B. Zhou, D.W. Williams, J. Altman, L.M. Riddiford, J.W. Truman, Temporal patterns of broad isoform expression during the development of neuronal lineages in *Drosophila*, Neural Dev. 4 (2009) 39.
[47] E.S. Belyaeva, M.G. Aizenzon, V.F. Semeshin, I.I. Kiss, K. Koczka, E.M. Baritcheva, T.D. Gorelova, I.F. Zhimulev, Cytogenetic analysis of the 2B3-4–2B11 region of the X-chromosome of *Drosophila melanogaster*. I. Cytology of the region and mutant complementation groups, Chromosoma 81 (1980) 281–306.
[48] I. Kiss, A.H. Beaton, J. Tardiff, D. Fristrom, J.W. Fristrom, Interactions and developmental effects of mutations in the Broad-Complex of *Drosophila melanogaster*, Genetics 118 (1988) 247–259.
[49] J.C. Fletcher, C.S. Thummel, The ecdysone-inducible Broad-Complex and E74 early genes interact to regulate target gene transcription and *Drosophila* metamorphosis, Genetics 141 (1995) 1025–1035.
[50] L.L. Restifo, K. White, Mutations in a steroid hormone-regulated gene disrupt the metamorphosis of the central nervous system in *Drosophila*, Dev. Biol. 148 (1991) 174–194.
[51] C.A. Bayer, L. von Kalm, J.W. Fristrom, Relationships between protein isoforms and genetic functions demonstrate functional redundancy at the Broad-Complex during *Drosophila* metamorphosis, Dev. Biol. 187 (1997) 267–282.
[52] R.F. Spokony, L.L. Restifo, Anciently duplicated Broad Complex exons have distinct temporal functions during tissue morphogenesis, Dev. Genes Evol. 217 (2007) 499–513.
[53] T.H. Morgan, C. Bridges, A.H. Sturtevant, The genetics of *Drosophila*, Bibliogr. Genet. 2 (1925) 145.
[54] J.W. Truman, L.M. Riddiford, The origins of insect metamorphosis, Nature 401 (1999) 447–452.
[55] J. Lubbock, On the Origin and Metamorphoses of Insects, Macmillan and Co., London, 1895.
[56] A. Berlese, Intorno alle metamorfosi degli insetti, Redia 9 (1913) 121–136.
[57] J.W. Truman, L.M. Riddiford, The morphostatic actions of juvenile hormone, Insect Biochem. Mol. Biol. 37 (2007) 761–770.
[58] W.C. Wheeler, M. Whiting, Q.D. Wheeler, J.M. Carpenter, The phylogeny of the extant hexapod orders, Cladistics 17 (2001) 113–169.

SUPPLEMENTARY DATA

Broad-complex functions in postembryonic development of the cockroach *Blattella germanica* shed new light on the evolution of insect metamorphosis

Jia-Hsin Huang, Jesus Lozano, Xavier Belles

CONTENTS

Supplementary Figure 1. Comparison of the joint expression of all BR-C isoforms, with the sum of the individual expression of the 6 isoforms, Z1 to Z6 represented in Figure 1C. Data are expressed as copies of BR-C mRNA per 1,000 copies of BgActin-5c.

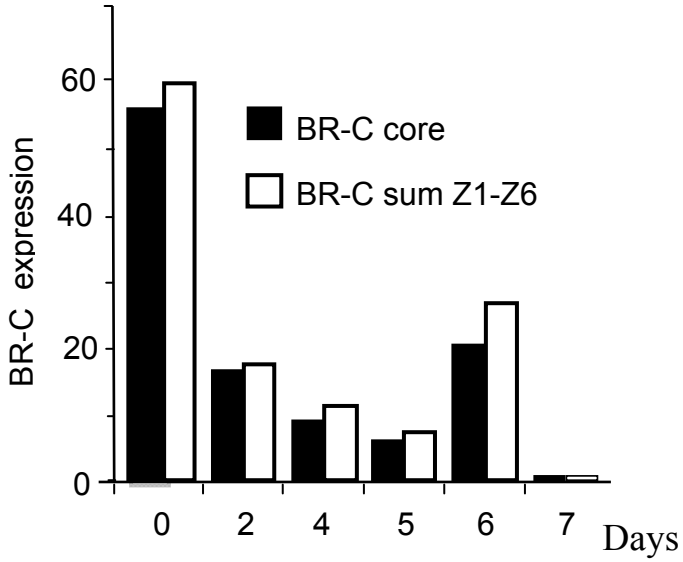

Supplementary Figure 2. Wings size of *Blattella germanica* resulting from a single dsBRCore treatment in N5 (treated) or from an equivalent treatment with dsMock (control). Top panel: Measurements carried out in the forewing (left) and hindwing (right). Bottom panel: data obtained; all values represent the mean ± SEM (n = 34 for treated, and n = 24 for controls); asterisks indicate statistically significant differences (* P < 0.01, ** P< 0.001, *t*-test).

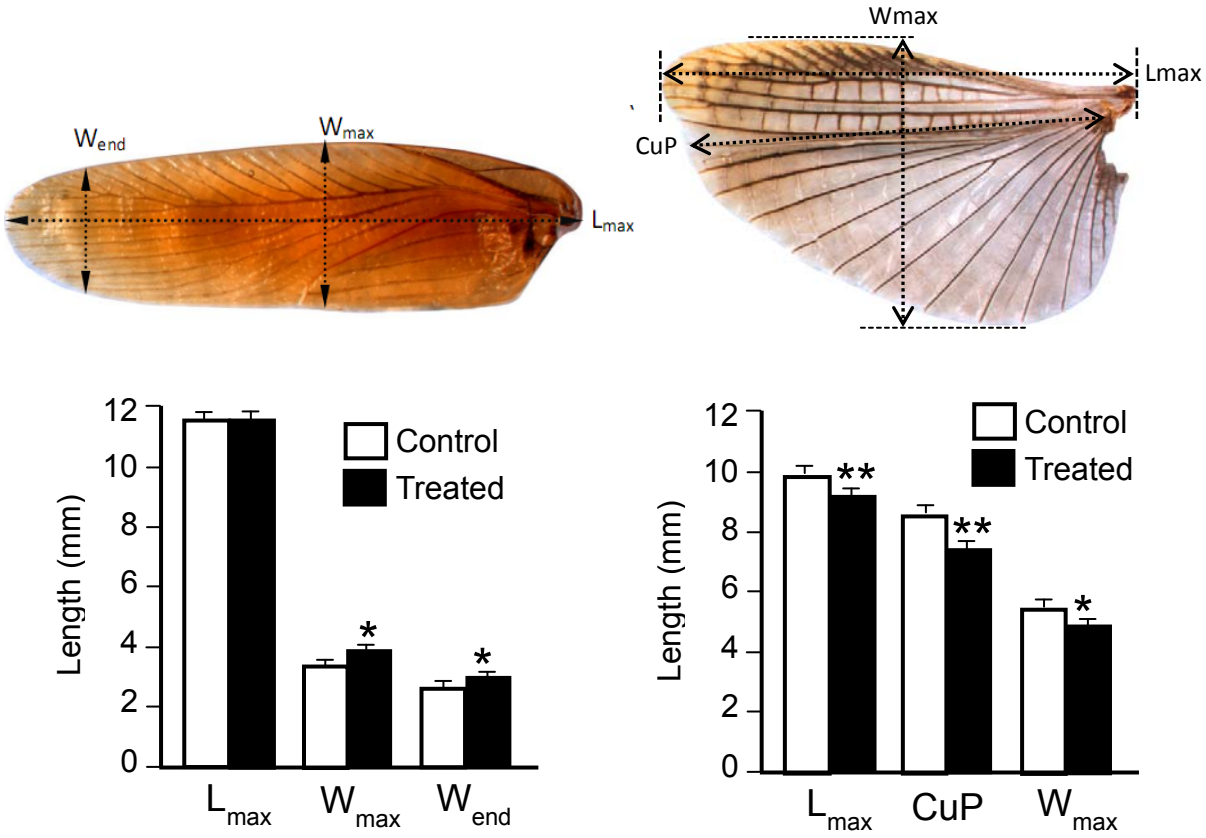

Supplementary Figure 3. Venation defects in the hind wing of *Blattella germanica* resulting from a single dsBRCore treatment in N5. Top panel: A, B and C, the three main defects observed. Bottom: penetrance of each defect or sum of defects in specimens treated with dsBRCore (treated) and in those treated with dsMock (controls).

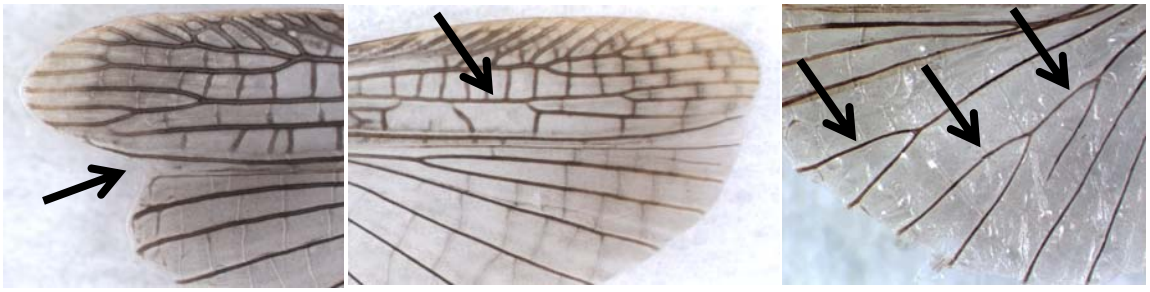

A: Short CuP (notch) B: Vein pattern disorganized C: A-veins broken

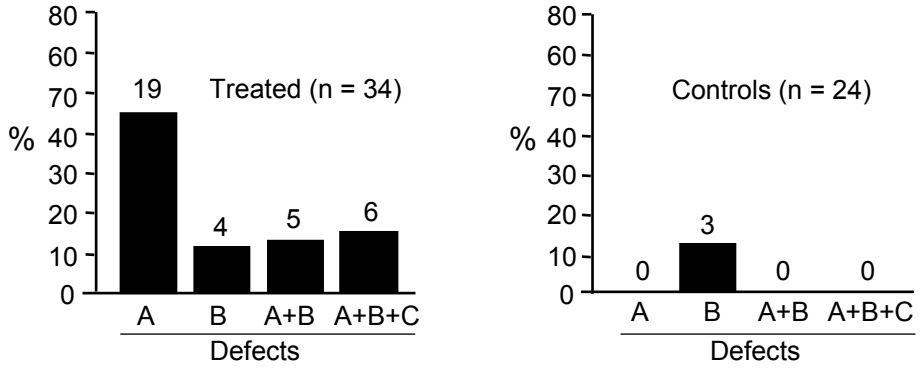

Supplementary Table 1. Primers used to detect the pool of all BR-C isoforms (BgBR-C) or to each isoform (BgBR-C Z1 to Z6). The accession numbers indicated in the "Encompassed region" column refer to the sequences of the different isoforms of *Blattella germanica* BR-C.

Primer set	Forward primer (5'-3')	Reverse primer (5'-3')	Encompassed region
BgBR-C	CGGGTCGAAGGGAAAGACA	CTTGGCGCCGAATGCTGCGAT	Nucleotide 699 to 774 of FN651774
BgBR-C Z1	CTTCAAGGGAGTACGGATGG	GGCGACGTAACCTCTGTAGC	Nucleotide 1298 to 1415 of FN651774
BgBR-C Z2	CTTCAAGGGAGTACGGATGG	ATGCTTGTCTGCAACGTGTC	Nucleotide 1298 to 1429 of FN651775
BgBR-C Z3	CTTCAAGGGAGTACGGATGG	TGGAGGAGGGATGCGATAAT	Nucleotide 1298 to 1372 of FN651776
BgBR-C Z4	CTTCAAGGGAGTACGGATGG	GAGAGGTAACTCGCCACTCG	Nucleotide 1298 to 1363 of FN651777
BgBR-C Z5	CTTCAAGGGAGTACGGATGG	GCAGTAAGGAGGTCCACTGC	Nucleotide 1298 to 1390 of FN651778
BgBR-C Z6	CTTCAAGGGAGTACGGATGG	CGCAGCTCATTTTGGATTTT	Nucleotide 1298 to 1398 of FN651779

Supplementary Table 2. Primers used to generate templates with PCR for transcription of dsRNAs designed to deplete all BR-C isoforms simultaneously (dsBrCore) or specific BR-C isoforms, BgBR-C Z1 to BgBR-C Z6 (dsBrZ1 to dsBrZ6). The accession numbers indicated in the "Encompassed region" column refer to the sequences of the different isoforms of *Blattella germanica* BR-C.

dsRNA	Length (bp)	Forward primer (5'-2')	Reverse primer (5'-3')	Encompassed region
dsBrCore	427	CATCAGAACAATCGCAGCATTC	TGTCCCTGAATACTGTCATGAAC	Nucleotide 744 to 1170 of FN651774
dsBrZ1	377	GCTCAGCAGGGACGTCAT	GATGAATTGAAACTTACTAACTCAAGG	Nucleotide 1317 to 1693 of FN651774
dsBrZ2	285	GCTCAGCAGGGACGTCAT	CACAGGTAACACCACCTTGGAAG	Nucleotide 1317 to 1601 of FN651775
dsBrZ3	411	GCTCAGCAGGGACGTCAT	TGTGTACATGAATGGATTTTTGG	Nucleotide 1317 to 1727 of FN651776
dsBrZ6	677	GCTCAGCAGGGACGTCAT	TCTTGCCATCATGATTAAATGAC	Nucleotide 1317 to 1993 of FN651777
dsBrZ4	612	GCTCAGCAGGGACGTCAT	AAATTTGATCATGGCCTTTG	Nucleotide 1317 to 1928 of FN651778
dsBrZ1	517	GCTCAGCAGGGACGTCAT	TTGCAACCAAATTCTTTAATAGG	Nucleotide 1317 to 1833 of FN651779